

# Metal-Oxicam Coordination Compounds: Structure, Biological Activity and Strategies for Administration

Gabriella Tamasi\*

Department of Chemistry, University of Siena, Via Aldo Moro 2, I-53100 Siena, Italy

**Abstract:** The crystal structures for metal-oxicam compounds published since the year 2000 are listed and commented in this review. The structural properties are interpreted in order to look for characteristics that might be significant for possible biological activities, for innovative strategies aimed to administering the metal based drugs *in vivo*. The relevant biological studies are also listed and commented. The number of structural reports on metal-oxicam compounds that were published up to the year 2000 was five, whereas the number of X-ray structures for the same class of compounds published since then is fifteen. The efforts carried out on the field during the past decade increased much and involved several research groups all over the world. The predominant metal was Cu<sup>II</sup>, but interest on Sn<sup>IV</sup> increased too, whereas the interest on Pt<sup>II</sup> continued for compounds derived from Zeise's salt. Other metals linked to oxicam ligands were investigated. The X-ray structural studies until ca ten years ago involved metal-piroxicam compounds, only; instead, during these past ten years also metal-meloxicam, -tenoxicam, -isoxicam, and -lornoxicam were studied and reported. The reactivity of cinnoxicam with copper(II)-acetate was also studied and reported. The coordination arrangement around Cu<sup>II</sup> showed a variety of modes that include *pseudo*-octahedral, -square planar, -square pyramidal. The oxicam coordination mode depends on the ligand, the reaction media and experimental conditions. The ligands usually occupy the equatorial positions of the coordination sphere and assume ZZZ conformations in the case they are in the anionic form (HOXI).

**Keywords:** Anti-inflammatory, Inflammation, X-ray crystallography, Complexes, Organo-metal compounds, Copper, Platinum, Cobalt, Zinc, Cadmium, Metal ion, Cytotoxic activity.

## 1. INTRODUCTION

Non-Steroidal Anti-Inflammatory Drugs (NSAIDs) from the oxicam family (See Scheme 1 for selected formulas) are still widely used to cure inflammations, and rheumatism in humans [1-4]. Several reports claimed that they have beneficial effects in preventing some forms of cancers when administered for prolonged periods [5-7]. Metal-NSAIDs complexes have been investigated for their improved curative effects in humans and animals [7]. Based on this rationale the search for metal-oxicam compounds was continued during recent years with renewed impetus, new data were collected on biological activity and new strategies for administering the new complexes were investigated and reported.

Reviews on metal-anti-inflammatory drugs have recently been published [7,8]. The field "anti-inflammatory compounds as ligands in metal complexes as revealed in X-ray structural studies" was reviewed and reported from this laboratory [9].

In the present review we wish to list and comment on the structures of metal-oxicam compounds that were not published at the time the review in Ref. [9] was written. Some biological properties of metal-oxicam complexes and possible innovative methods aimed to administer the metal based potential drugs *in vivo* are also commented. The compounds

are classified into two parts: (a) organo-metal compounds (that contain at least a metal-carbon bond), and (b) Werner coordination compounds.

## 2. ORGANO-METAL COMPOUNDS

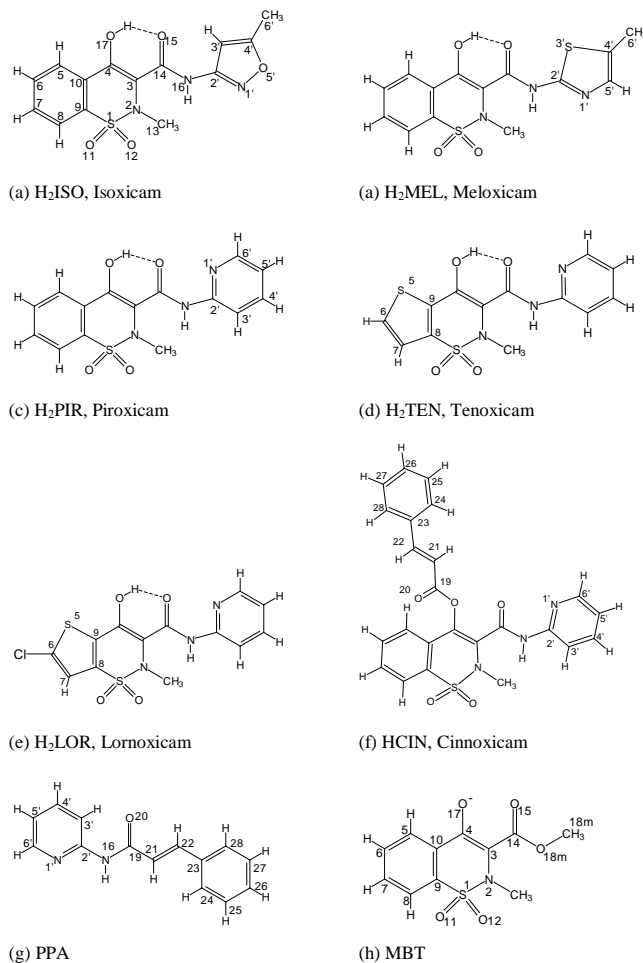
A list of compounds published after the year 2000, not reported in the review in Ref. [9], as well as of selected major information for their preparation is reported in Table 1.

### 2.1. Synthetic Procedures

The crystalline organo-Sn<sup>IV</sup> compounds [Sn<sup>IV</sup>(*Q,N,N'*-TEN)(n-Bu)<sub>2</sub>], **1** [10] and [Sn<sup>IV</sup>(*Q,N,N'*-LOR)(R)<sub>2</sub>], (R = n-Bu, **3**; R = Me, **4**) [11] were usually obtained by refluxing a solution of the relevant oxicam ligand and Sn<sup>IV</sup>R<sub>2</sub>O (Sn:H<sub>2</sub>OXI, 1:1 molar ratio, in benzene). The clear solutions were brought to dryness and the residues were re-dissolved in MeOH (**1**) or hexane (**3**) or Et<sub>2</sub>O (**4**). On slowly evaporating the solvent the pale yellow crystalline compounds that formed were collected through filtration. In the synthesis of **3** and **4** the yellow solid that formed was dissolved in Et<sub>2</sub>O and the procedure described above was repeated twice. Finally, single crystals suitable for X-ray diffraction (XRD) studies were obtained *via* re-crystallization from mixtures of solvents (MeOH/CH<sub>3</sub>CN, **1**; Et<sub>2</sub>O/CH<sub>2</sub>Cl<sub>2</sub>, **3**; C<sub>6</sub>H<sub>12</sub>/C<sub>6</sub>H<sub>6</sub>, **4**).

Noteworthy, Ref. [10] reports the preparation of [Sn<sup>IV</sup>(HTEN)<sub>2</sub>(n-Bu)<sub>2</sub>], **2**, by following a procedure similar to that for **1** but using a H<sub>2</sub>TEN:Sn, 2:1 molar ratio in the

\*Address correspondence to this author at the Department of Chemistry, University of Siena, Via Aldo Moro 2, I-53100 Siena, Italy; Tel: +39 0577 234368; Fax: +39 0577 234254, E-mail: tamasi@unisi.it



**Scheme 1.** The drawings show the structural formulas for: **(a)** H<sub>2</sub>ISO, **(b)** H<sub>2</sub>MEL, **(c)** H<sub>2</sub>PIR, **(d)** H<sub>2</sub>TEN, **(e)** H<sub>2</sub>LOR, **(f)** HCIN, **(g)** PPA, **(h)** MBT.

**Table 1.** Crystalline Metal-Oxicam Compounds Commented in this Review

Compounds	Preparation Medium	Ref.	CSD Code <sup>a</sup>
<b>Organo-metal compounds</b>			
[Sn <sup>IV</sup> ( <i>Q,N,N'</i> -TEN)(n-Bu) <sub>2</sub> ], <b>1</b>	C <sub>6</sub> H <sub>6</sub> /CH <sub>3</sub> OH/CH <sub>3</sub> CN	[10]	QAJTEA
[Sn <sup>IV</sup> ( <i>Q,N,N'</i> -LOR)(n-Me) <sub>2</sub> ], <b>3</b>	C <sub>6</sub> H <sub>6</sub> /C <sub>2</sub> H <sub>5</sub> OC <sub>2</sub> H <sub>5</sub> /CH <sub>2</sub> Cl <sub>2</sub>	[11]	EHIGUX
[Sn <sup>IV</sup> ( <i>Q,N,N'</i> -LOR)(n-Bu) <sub>2</sub> ], <b>4</b>	C <sub>6</sub> H <sub>6</sub> /C <sub>6</sub> H <sub>12</sub> /C <sub>2</sub> H <sub>5</sub> OC <sub>2</sub> H <sub>5</sub>	[11]	EHIGOR
<i>trans</i> -[Pt <sup>II</sup> ( <i>N,N'</i> -H <sub>2</sub> TEN)Cl <sub>2</sub> (η <sup>2</sup> -C <sub>2</sub> H <sub>4</sub> )], <b>5</b>	C <sub>2</sub> H <sub>5</sub> OH/C <sub>6</sub> H <sub>6</sub>	[12]	UHIMIH
<i>trans</i> -[Pt <sup>II</sup> ( <i>N,N'</i> -H <sub>2</sub> MEL)Cl <sub>2</sub> (η <sup>2</sup> -C <sub>2</sub> H <sub>4</sub> )], <b>6</b>	C <sub>2</sub> H <sub>5</sub> OH/CHCl <sub>3</sub>	[12]	UHIMON
<i>cis</i> -[Sn <sup>IV</sup> ( <i>Q,Q'</i> -PIR) <sub>2</sub> (η <sup>1</sup> -C <sub>6</sub> H <sub>5</sub> ) <sub>2</sub> ], <b>7</b>	H <sub>2</sub> O/CH <sub>3</sub> OH/CH <sub>3</sub> CN	[13]	RAFRIA
<b>Werner complexes</b>			
<i>trans</i> -[Co <sup>II</sup> ( <i>Q,N'</i> -HMEL) <sub>2</sub> ( <i>Q</i> -DMSO) <sub>2</sub> ], <b>8</b>	CH <sub>3</sub> OH/(CH <sub>3</sub> ) <sub>2</sub> SO	[14]	CAKLOQ
<i>trans</i> -[Zn <sup>II</sup> ( <i>Q,N'</i> -HMEL) <sub>2</sub> ( <i>Q</i> -DMSO) <sub>2</sub> ], <b>9</b>	CH <sub>3</sub> OH/(CH <sub>3</sub> ) <sub>2</sub> SO	[14]	CAKLUW
<i>trans</i> -[Cd <sup>II</sup> ( <i>Q,N'</i> -HMEL) <sub>2</sub> ( <i>Q</i> -DMSO) <sub>2</sub> ], <b>10</b>	CH <sub>3</sub> OH/(CH <sub>3</sub> ) <sub>2</sub> SO	[14]	CAK MAD
<i>trans</i> -[Cd <sup>II</sup> ( <i>Q,N'</i> -HTEN) <sub>2</sub> ( <i>Q</i> -DMSO) <sub>2</sub> ], <b>11</b>	CH <sub>3</sub> OH/(CH <sub>3</sub> ) <sub>2</sub> SO	[12]	UHIMED
<i>trans</i> -[Cu <sup>II</sup> ( <i>Q,N'</i> -HTEN) <sub>2</sub> (PY) <sub>2</sub> ], <b>12</b>	C <sub>5</sub> H <sub>5</sub> N/C <sub>2</sub> H <sub>5</sub> OH	[15]	-
[Cu <sup>II</sup> ( <i>Q,Q'</i> -HISO)( <i>Q,N'</i> -HISO)]·0.5DMF, <b>13</b>	CH <sub>3</sub> OH/(CH <sub>3</sub> ) <sub>2</sub> NCHO	[16]	CIHZID
[Cu <sup>II</sup> ( <i>Q,N'</i> -HMEL) <sub>2</sub> ( <i>Q</i> -DMF)]·0.25H <sub>2</sub> O, <b>14</b>	CH <sub>3</sub> OH/(CH <sub>3</sub> ) <sub>2</sub> NCHO	[16]	CIHZOJ
<i>trans</i> -[Cu <sup>II</sup> ( <i>Q,Q'</i> -MBT) <sub>2</sub> ( <i>N</i> -PPA) <sub>2</sub> ], <b>15</b>	CH <sub>3</sub> OH/(CH <sub>3</sub> ) <sub>2</sub> NCHO	[16]	CIHZUP
<i>trans</i> -[Cu <sup>II</sup> ( <i>Q,N'</i> -HPIR) <sub>2</sub> ( <i>Q</i> -DMSO) <sub>2</sub> ], <b>16</b>	CH <sub>3</sub> OH/(CH <sub>3</sub> ) <sub>2</sub> SO	[17]	CSD 684972
<i>trans</i> -[Cu <sup>II</sup> ( <i>Q,N'</i> -HISO) <sub>2</sub> ( <i>Q</i> -THF) <sub>2</sub> ], <b>17</b>	CH <sub>3</sub> OH/(CH <sub>3</sub> ) <sub>2</sub> NCHO/(CH <sub>2</sub> ) <sub>4</sub> O	[17]	CSD 684973

<sup>a</sup>Ref. [18].

starting mixture (benzene). The paper in Ref. [10] states that the slow evaporation of a solution of **2** in MeOH/CH<sub>3</sub>CN yielded **1** as pale yellow crystals and H<sub>2</sub>TEN (powder).

The crystalline organo-Pt<sup>II</sup> compounds, *trans*-[Pt<sup>II</sup>(N<sup>1</sup>-H<sub>2</sub>OXI)Cl<sub>2</sub>(η<sup>2</sup>-C<sub>2</sub>H<sub>4</sub>)], (H<sub>2</sub>OXI = H<sub>2</sub>TEN, **5**; H<sub>2</sub>OXI = H<sub>2</sub>MEL, **6**) [12] were obtained *via* a general procedure that consisted of mixing the two freshly prepared solutions of the oxicam ligand (in EtOH under stirring at 60°C) and of K[PtCl<sub>3</sub>(η<sup>2</sup>-C<sub>2</sub>H<sub>4</sub>)]·H<sub>2</sub>O (Zeise's salt, in EtOH at room temperature) and on stirring the final mixture at room temperature. A pale yellow micro-crystalline solid precipitates that was collected and finally re-crystallized from benzene (**5**) and from chloroform (**6**).

The crystalline organo-Sn<sup>IV</sup> compound, *cis*-[Sn<sup>IV</sup>(*Q,Q'*-PIR)<sub>2</sub>(η<sup>1</sup>-C<sub>6</sub>H<sub>5</sub>)<sub>2</sub>], (**7**) [13] was prepared by adding a suspension of H<sub>2</sub>PIR in water to a solution of KOH (1:1 molar ratio), and the resulting solution was mixed with Sn<sup>IV</sup>Cl<sub>2</sub>Ph<sub>2</sub> in MeOH under stirring (Sn:HPIR<sup>-</sup>, molar ratio 1:2). The crude solid product was re-crystallized from MeOH/CH<sub>3</sub>CN that produced single crystals of the acetonitrile solvate of **7**.

To summarize, the number of organo-metal compounds that contain any NSAIDs from the oxicam family so far reported is small; notwithstanding, the synthetic strategies just listed are easy to perform, and produce crystalline materials in high yields. It is reasonable to expect that attempts to prepare other complexes from the oxicam ligands with other metal cations will be successful. Forthcoming studies should also be devoted to search for metal compounds significantly soluble in aqueous media in order to allow the determination of biological activity and of reactivity with bio-molecules.

## 2.2. Structures of the Anti-Inflammatory Drug – Organo Metal Compounds

### 2.2.1. The Sn<sup>IV</sup> Derivatives

The structures of **1** [10], **3** and **4** [11] have a pattern similar to that reported previously for [Sn<sup>IV</sup>(*Q,N,N'*-PIR)(n-Bu)<sub>2</sub>] [19]. The OXI<sup>2-</sup> anions for the three compounds show a *Q,N,N'* coordination mode. Instead, the structure for **7** shows a *Q,Q'* chelating scheme.

#### 2.2.1.1. The Coordination Sphere

The TEN<sup>2-</sup> ligand for **1** is coordinated to the Sn<sup>IV</sup> center *via* enolato oxygen, amidato nitrogen and pyridyl nitrogen atoms (Fig. 1). The two carbon atoms from n-Bu groups complete the five sites of square-pyramidal coordination arrangement around the tin atom. The strong affinity of Sn<sup>IV</sup> centers for oxygen donors is in agreement with the short Sn-O(enolato) bond distance (2.094(3) Å), that has to be compared to the significantly longer Sn-N(amide) (2.159(3) Å) and Sn-N(pyridyl) (2.426(3) Å) bond distances. A weak Sn...O(amide) interaction (Sn-O, 2.650(4) Å) links a complex molecule to another one, so that chains of (amide)O...Sn-N(amide)-C-O(amide)...Sn bonds exist at the solid state. The Sn-C bond distances (2.117(4) Å, average) are in agreement with other organo-tin bonds and with the corresponding structure for the homologous PIR<sup>2-</sup> derivative [8,19].

The structure of **4** has Sn-O(enolato), Sn-N(amide), Sn-N(pyridyl) and Sn-C bond distances 2.110(8), 2.137(8), 2.399(8), 2.111(4) Å (average), respectively, that compare

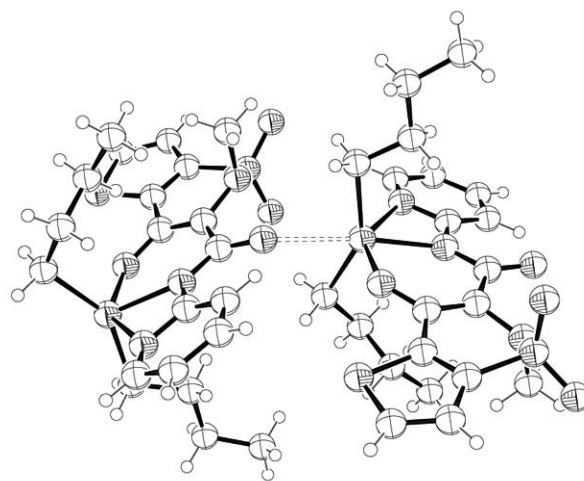


**Fig. (1).** Structure of two molecules of [Sn<sup>IV</sup>(*Q,N,N'*-TEN)(n-Bu)<sub>2</sub>], **1**, (CSD code, QAJTEA). Molecule on the left *x,y,z*; molecule on the right  $-x+0.5, -y+0.5, z+0.5$ .

well with the values for the analogous species **1** commented above. The Sn...O(amide) contact distance is 2.96(1) Å, much higher than that found for the TEN<sup>2-</sup> derivative. Therefore, it has to be noted that the formation of aggregates through this type of Sn...O(amide) bond is typical in this class of compound but the strength of the interaction depends on the type of ligand and spans a wide range of contact distances.

In the case of the structure for **3** (Fig. 2) the main coordination arrangement around the tin center is maintained unaltered with respect to **1** and **4**. The Sn-O(enolato), Sn-N(amidate), Sn-N(pyridyl) and Sn-C bond distances are 2.094(4), 2.119(4), 2.400(4), and 2.107(5) (average) Å, respectively. In this case the associations of complex molecules *via* Sn...O interaction is very weak; intra-molecular

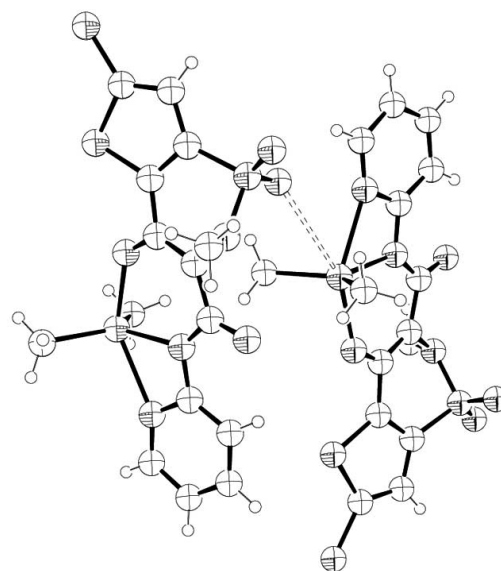


**Fig. (2).** Structure of two molecules of [Sn<sup>IV</sup>(*Q,N,N'*-LOR)(n-Me)<sub>2</sub>], **3** (CSD code, EHIGUX). Molecule on the left *x,y,z*; molecule on the right  $-x+2, y+0.5, -z+2$ .

Sn...O interaction (3.56(1) Å) involves an oxygen atom from the SO<sub>2</sub> function. It is noteworthy that the C-Sn-C bond angle is 126.1(2)°, much lower than the values found for the n-Bu derivatives (147.5(4)° **1**, 141.1(4)° **4**), and 144.7(4)° [Sn<sup>IV</sup>(*Q,Q',N*-PIR)(n-Bu)<sub>2</sub>] [19].

The structure of **7** (Fig. 3) has the Sn<sup>IV</sup> metal ion at the center of an octahedral arrangement that consists of two HPIR<sup>-</sup> anion chelating *via* the enolato and amide oxygen atoms. The amide nitrogen does not act as a donor to the metal and retains its hydrogen; this is in contrast with what found for the analogous di-*n*-butyl derivative. The coordination sphere is completed by two η<sup>1</sup>-phenylate ligands that occupy *cis* positions. The coordination linkages to the enolato oxygen atoms (2.105(3) Å, average) are significantly shorter than those to amide oxygen atoms (2.194(3) Å, average). The O(enolato)-Sn-O(amide) bond angles from different ligand molecules are narrow and average 79.7(6)°. Even the O-Sn-O chelating angles are narrow and average 80.8(6)°. The C-Sn-C and C-Sn-O(enolato) bond angles are in the range 96.7(6) – 107.4(6)°.

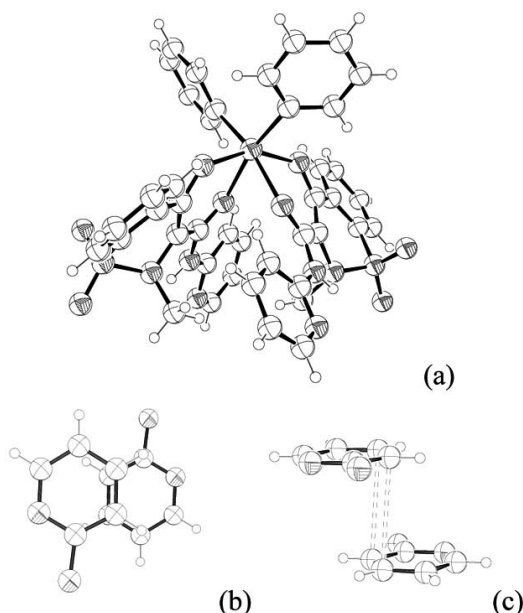


**Fig. (3).** (a) Structure of *cis*-[Sn<sup>IV</sup>(*Q,Q'*-PIR)<sub>2</sub>(η<sup>1</sup>-C<sub>6</sub>H<sub>5</sub>)<sub>2</sub>], **7** (CDS code, RAFRIA). Inter-molecular stacking interaction between amido-pyridyl functions: (b) as viewed along the normal planes; (c) as viewed almost parallel to the planes.

### 2.2.1.2. The Oxicam Ligand

The OXI<sup>2-</sup> ligands for **1**, **3** and **4** have ZZE conformations. The selected structural parameter for the complexes are listed in Table 2.

The bond distances for the atoms of the enolato-amide-pyridyl system do not change significantly in the three complexes, even though the Sn-N(amidato) bond distance is different for **1** and **3**, and the Sn...O(amidato) inter-molecular contact distance undergoes significant changes for the three compounds: 2.650(4) Å **1**, 4.20(1) Å **3**, 2.96(1) Å **4**. Similarly, the bond angles for the O17-C4-C3-C14(O15)-N16-C2' chain do not change significantly within the series **1**, **3**, **4**. The N1'-C2'-N16 bond angles span a narrow range

(107.8(5) – 108.6(4)°) and is in agreement with formation of the four member chelate ring Sn-N16-C2'-N1' and with the corresponding value found for [Sn<sup>IV</sup>(*Q,Q',N*-PIR)(n-Bu)<sub>2</sub>] (108.4(5)°) [19]. The analysis of the torsion angles shows that **3** has an almost planar enolato-amidato-pyridyl system (O17-C4-C3-C14, ω<sub>17</sub>, -0.6(4)°; C4-C3-C14-N16, ω<sub>4</sub>, -1.5(4)°); whereas, **1** and **4** have a larger deviation from planarity (ω<sub>17</sub>, -6.7(4)° **1** and -7.0(6)° **4**; ω<sub>4</sub>, -7.2(4)° **1** and -7.9(6)° **4**). The deviation from planarity could be in part due to the steric hindrance from the bulky n-Bu ligands (**1** and **4**) when compared to the smaller Me ligand (**3**). The torsion angles at the thieno-thiazine systems are close to each other for **1**, **3**, **4**. For example angle C9-C8-S1-N2, τ<sub>9</sub>, is -34.1(4)° **1**, -31.8(4)° **3** and -32.2(7)° **4**. The corresponding value for the benzo-thiazine system C10-C9-S1-N2, τ<sub>10</sub>, is -36.8(4)° for [Sn<sup>IV</sup>(*Q,Q',N*-PIR)(n-Bu)<sub>2</sub>] [19].

The conformation of the HOXI<sup>-</sup> ligands for **7** is the somewhat unusual EZE when compared to the preferred ZZZ one. It has to be recalled that the preparation was performed in aqueous solution by mixing H<sub>2</sub>PIR, Ph<sub>2</sub>SnCl<sub>2</sub> and KOH in a 2:1:2 molar ratio. It seems that the high affinity of tin for oxygen atoms when compared to nitrogen donors plays a significant role in this coordination mode. The bond distances at the enolato-amide-pyridyl system for **7** are close to those for **1**, **3**, **4** (once the estimated standard deviations are taken into account). Instead, the bond angles for **7** have significant changes with respect to the corresponding values for **1**, **3**, **4**. In fact, C4-C3-C14 undergoes a narrowing from 127.7(4)-129.0(4)° (**1**, **3**, **4**) to 123.4(7)° (**7**); C14-N16-C2' and N16-C2'-N1' undergo a widening from 122.6(6)-123.1(5)° (**1**, **3**, **4**) to 129.8(7)° (**7**) and 107.8(6)° - 108.6(5)° (**1**, **3**, **4**) to 113.3(7)° (**7**). Deviations from planarity of enolato-amide-pyridyl system as measured by the ω<sub>3</sub>, ω<sub>4</sub>, ω<sub>15</sub>, ω<sub>17</sub> torsion angles are similar to that for the **1**, **4** species and hence higher than those for **3**. The ω<sub>14</sub> torsion angle has very close values for **1**, **3**, **4** and **7**.

### 2.2.1.3. Intra- and Inter-Molecular Weak Interactions

Compounds **1**, **3** and **4** show a weak intra-molecular (pyridyl)C-H...O(amide) H-bond type interaction with C...O contact distances and Ĥ angles in the range 2.83(1) – 3.07(1) Å and 116(1) -117(1)°. Short contact distances between certain H-atoms from the n-Bu chains and the C4-C3-C14-N16 (plane π<sub>4</sub>) atoms were detected for **1** and **4**. The orientation of n-Bu chains and several short (C)H...π shows distances in the range 2.46(1) – 2.76(1) Å suggesting that (C)H...π linkages occur. It has to be noted that H...π distances in the range 2.43(1) - 2.59(1) Å could be detected in organo-rhodium molecules in both solid and solution phases [20].

It has to be noted that for **7** the commonly found (see Werner complexes, below) and stabilizing O(enolato)...H-N(amide) hydrogen bond is not present. Weak N-H...N(CH<sub>3</sub>) hydrogen bonds exist (N...N, 2.70(1) Å; Ĥ, 110(2)° average). Noteworthy, the two mean oxicam planes (that have a head-to-tail arrangement) are tilted towards each other with respect to the Sn-O lines. The narrow dihedral angle between the mean planes defined by the non-hydrogen atoms of enolato-amide-pyridyl functions (54.4(8)°) **7** can be tentatively related to several intra-molecular effects and possibly even to inter-molecular forces.

**Table 2.** The Selected Bond Distances (Å) and Bond Angles (°) within the OXI<sup>2-</sup> Ligands for some Organo-Sn<sup>IV</sup> Compounds. Estimated Standard Deviations are in the Ranges: 1 and 3, 0.004-0.005 Å and 0.4-0.5°; 4 and 7, 0.006-0.007 Å and 0.6-0.7°. The CSD [18] Code is also Reported

Parameter	1, QAJTEA	3, EHIGUX	4, EHIGOR (Average)	7, RAFRIA (Average)
<b>Distances</b>				
O17-C4	1.309	1.315	1.328	1.301
C4-C3	1.371	1.358	1.374	1.379
C3-C14	1.474	1.474	1.475	1.445
C14-O15	1.232	1.221	1.248	1.256
C14-N16	1.359	1.365	1.380	1.354
N16-C2'	1.395	1.395	1.400	1.421
<b>Angles</b>				
O17-C4-C3	128.0	127.9	127.0	126.0
C4-C3-C14	127.7	129.0	128.2	123.4
C3-C14-O15	120.9	121.4	119.5	123.5
C3-C14-N16	115.8	115.8	115.0	117.5
O15-C14-N16	123.3	122.9	125.3	119.0
C14-N16-C2'	123.1	124.1	122.6	129.8
N16-C2'-N1'	108.0	108.6	107.8	113.3
<b>Torsion angles</b>				
O17-C4-C3-C14, $\omega_{17}$	-6.7	-0.6	-6.7/-7.3	-4.0/-0.7
O15-C14-N16-C2', $\omega_{15}$	7.0	0.5	11.2/7.8	10.1/1.2
C14-N16-C2'-N1', $\omega_{14}$	-175.2	172.8	173.6/175.7	178.3/168.9
C4-C3-C14-N16, $\omega_4$	-7.2	-1.5	-7.2/-8.5	-169.3/174.4
C3-C14-N16-C2', $\omega_3$	-171.3	-179.0	-171.1/175.7	-169.7/178.3

Attractive C-H... $\pi$  intra-molecular interactions between (N)CH<sub>3</sub> and pyridyl functions are detected, shortest (C)H... $\pi$  2.72(1) Å. It has to be noted that even repulsive interactions between Ph atoms and piroxicam atoms as well as other attractive forces between the two HPIR<sup>-</sup> ligands can contribute to the tilting of the two HPIR<sup>-</sup>  $\pi$  mean planes towards each other.

Selected inter-molecular interactions (excluding the Sn...O ones above commented) for **1** are (pyridyl)C-H...O(SO<sub>2</sub>) interactions (C...O 3.58(1) Å,  $\hat{H}$  141(2)°). Hydrogen bond type interactions (pyridyl)C-H...O(SO<sub>2</sub>) contribute to link two complex molecules in **4** (C...O 3.32(1) Å,  $\hat{H}$  134(2)°). The chlorine atom from LOR<sup>2-</sup> in **4** is surrounded by several H-atoms from several groups. The selected H-bonds being (n-Bu)C1-H...Cl (C...Cl 3.84(1) Å,  $\hat{H}$  153(2)°), and (NCH<sub>3</sub>)C-H...Cl (C...Cl, 3.85(1) Å,  $\hat{H}$  156(2)°). Methyl ligands for **3** are also involved in C-H...O(SO<sub>2</sub>) H-bond inter-molecular interactions (C...O 3.32(1) Å,  $\hat{H}$  142(2)°). The sulfur dioxide group is also acceptor from (pyridyl)C-H functions (C...O 3.07(1) Å,  $\hat{H}$  130(2)°). Weak intra-molecular stacking interactions involve the thieno and pyridyl systems (shortest contact, C...C

3.51(1) Å with a poor overlap of planes for the structure of **1**. The structure for **3** has extensive thieno-pyridyl stacking interaction with significant overlap and several short C...C contacts (3.54(1) Å). The structure for **7** shows small overlap but short contact (3.45(1) Å) stacking interactions between pyridyl systems.

### 2.2.2. The Pt<sup>II</sup> Derivatives

The structures for **5** and **6** are similar to those previously reported for the analogous ethene and DMSO [9,21,22] derivatives that contain H<sub>2</sub>PIR.

#### 2.2.2.1. The Coordination Sphere

The structure of **5** has the square-planar Pt<sup>II</sup> center linked to a H<sub>2</sub>TEN molecule through the pyridyl nitrogen atom and to the  $\eta^2$ -ethene molecule (*trans* to each other). The coordination sphere is completed by the two chlorido donors. The Pt-N1', Pt-Cl and Pt-C bond distances are 2.078(5), 2.267(2) (average) and 2.151(7) Å (average), respectively.

The structure for **6** is similar to that for the H<sub>2</sub>TEN derivative as regards the main features. The coordination sphere includes thiazolyl nitrogen atom, the  $\eta^2$ -ethene mole-

cule (*trans* to each other) as well as the two chlorido donors. The Pt-N1', Pt-Cl and Pt-C bond distances are 2.072(3), 2.300(6) (average) and 2.135(7) Å (average), respectively.

### 2.2.2.2. The Oxicam Ligand

The selected structural parameter for the molecules **5** and **6** are listed in Table 3. The oxicam ligand mean plane is tilted with respect to the coordination plane. In fact, the narrowest Cl-Pt-N1'-C2' torsion angle is 72.9(3)° for the H<sub>2</sub>TEN derivative and 59.6(7)° for the H<sub>2</sub>MEL one. The dihedral angle between the N16-pyridyl/N16-thiazolyl mean planes and coordination plane defined by N1' and Cl donors is 74.4(4)° **5** and 56.1(8)° **6** (67.2(4)°, [Pt(N<sup>1'</sup>-H<sub>2</sub>PIR)Cl<sub>2</sub>(η<sup>2</sup>-C<sub>2</sub>H<sub>4</sub>)] [21] and 78.5(4)/80.5(4)° for [Pt(N<sup>1'</sup>-H<sub>2</sub>PIR)Cl<sub>2</sub>(DMSO)] [22]).

**Table 3.** The Selected Bond Distances (Å) and Bond Angles (°) within the H<sub>2</sub>OXI Ligands for **5** and **6**. Estimated Standard Deviations are in the Ranges: 0.006-0.020 Å and 0.4-1.0°. The CSD [18] Code is also Reported

Parameter	5, UHIMIH	6, UHIMON
<b>Distances</b>		
O17-C4	1.340	1.359
C4-C3	1.363	1.33
C3-C14	1.452	1.49
C14-O15	1.226	1.226
C14-N16	1.368	1.35
N16-C2'	1.381	1.40
<b>Angles</b>		
O17-C4-C3	123.9	122.3
C4-C3-C14	121.6	122.5
C3-C14-O15	122.1	121.6
C3-C14-N16	113.9	114.7
O15-C14-N16	124.0	123.1
C14-N16-C2'	129.7	125.4
N16-C2'-N1'	114.6	120.6
<b>Torsion angles</b>		
O17-C4-C3-C14, ω <sub>17</sub>	0.7	-5
O15-C14-N16-C2', ω <sub>15</sub>	-3.3	0
C14-N16-C2'-N1', ω <sub>14</sub>	-166.7	-159
C4-C3-C14-N16, ω <sub>4</sub>	172.7	-163
C3-C14-N16-C2', ω <sub>3</sub>	177.8	171
Cl-Pt-N1'-C2'	-72.9	-60

The conformation at the enol-amide-pyridyl chain is EZE for **5** and **6**. Corresponding bond lengths and bond angles for the H<sub>2</sub>TEN and H<sub>2</sub>MEL ligands are equal within the esds. Instead, the torsion angles for the two molecules show significant differences (see Table 3). H<sub>2</sub>MEL ligand in **6** is

less planar than H<sub>2</sub>TEN in **5**. Torsion angle ω<sub>14</sub> (C14-N16-C2'-N1') deviates significantly from 180° for both compounds; **6** has higher deviation (21(1)°) than for **5** (13.3(5)°). Noteworthy, the deviation for H<sub>2</sub>PIR in [Pt(N<sup>1'</sup>-H<sub>2</sub>PIR)Cl<sub>2</sub>(η<sup>2</sup>-C<sub>2</sub>H<sub>4</sub>)] is also high (ω<sub>14</sub> 28.2(4)° [21]; whereas for H<sub>2</sub>PIR in [Pt(N<sup>1'</sup>-H<sub>2</sub>PIR)Cl<sub>2</sub>(DMSO)] [22] the situation is similar to that for **5**. In conclusion the flexibility of the enol-amide-pyridyl/thiazolyl system does not depend much on the nature of H<sub>2</sub>OXI ligand but from nature of other ligands and packing forces.

### 2.2.2.3. Intra- and Inter-Molecular Weak Interactions

The ligand molecule is stabilized *via* a strong intra-molecular O(enol)-H...O(amide) hydrogen bond (O...O, 2.633(8) Å **5** and 2.62(2) Å **6**). The Pt...H-N(amide) contact distance is 2.54(1) Å in the complex **5**, suggesting a significant electrostatic (possibly anagostic-like) interaction that involves the N-H function and the metal center. Similar facts were found and reported previously for [Pt(N<sup>1'</sup>-H<sub>2</sub>PIR)Cl<sub>2</sub>(η<sup>2</sup>-C<sub>2</sub>H<sub>4</sub>)] [21] and [Pt(N<sup>1'</sup>-H<sub>2</sub>PIR)Cl<sub>2</sub>(DMSO)] [22]. In the case of **6** the interaction is much weaker (Pt...HN, 2.93(2) Å) whereas an intra-molecular N-H...Cl interaction is significant N...Cl 3.25(2) Å, ∠ 144(2)°.

Inter-molecular H-bond interactions involve SO<sub>2</sub> groups as acceptors from C-H functions from thieno rings (shortest C...O 3.25(1) Å, ∠ 164(2)° for **5**). Chlorido donors in **5** are involved in weak C-H...Cl H-bonds, and accepting from pyridyl CH and NCH<sub>3</sub> functions. Sulfur dioxide accepts hydrogen atoms from (N)CH<sub>3</sub> and (thiazolyl)CH<sub>3</sub> groups in the structure of **6**. Chlorido donors accept hydrogen from ethene ligands.

Stacking π...π interactions exist between amide function and pyridyl system in the structure for **5** for which short contacts of the type (pyridyl)C...C(O), ...N, and ...O were detected (3.39(1), 3.37(1) and 3.69(1) Å). Stacking π...π interactions exist also in the structure for **6** between thiazoyl-amide system and benzo-enol system of the H<sub>2</sub>MEL ligands. The overlap of π systems is limited but contact distances are small: C...C and C...S 3.55(3) Å and 3.59(2) Å, and this suggests that attractive interactions between planes play a role.

## 3. WERNER COMPOUNDS

The list of Werner compounds appeared after the year 2000, not commented in Ref. [9], and the selected major information for their preparation is reported in Table 1.

### 3.1. Synthetic Procedures

The preparation methodology was mainly the same for the complexes: *trans*-[Co<sup>II</sup>(Q,N'-HMEL)<sub>2</sub>(Q-DMSO)<sub>2</sub>], **8**; *trans*-[Zn<sup>II</sup>(Q,N'-HMEL)<sub>2</sub>(Q-DMSO)<sub>2</sub>], **9**; *trans*-[Cd<sup>II</sup>(Q,N'-HMEL)<sub>2</sub>(Q-DMSO)<sub>2</sub>], **10** [14]; *trans*-[Cd<sup>II</sup>(Q,N'-HTEN)<sub>2</sub>(Q-DMSO)<sub>2</sub>], **11** [12]; [Cu<sup>II</sup>(Q,Q'-HISO)(Q,N'-HISO)]·0.5 DMF, **13**; [Cu<sup>II</sup>(Q,N'-HMEL)<sub>2</sub>(Q-DMF)]·0.25H<sub>2</sub>O, **14** [16]; *trans*-[Cu<sup>II</sup>(Q,N'-PIR)<sub>2</sub>(Q-DMSO)<sub>2</sub>], **16**; *trans*-[Cu<sup>II</sup>(Q,N'-HISO)<sub>2</sub>(Q-THF)<sub>2</sub>], **17** [17]. A clear alcoholic solution of the metal acetate was added to a warm alcoholic (usually MeOH) solution of the oxicam ligand (metal:ligand, 1:2 molar ratio). The resulting mixture was refluxed under stirring and the micro-crystalline product was collected. Finally, single crystals suitable for XRD studies were

obtained through re-crystallization (**8-11**, and **16** from DMSO; **13** and **14** from DMF; and **17** from THF).

The complex *trans*-[Cu<sup>II</sup>(*Q,N'*-HTEN)<sub>2</sub>(PY)<sub>2</sub>], **12** was prepared through a slightly different procedure. A solution of H<sub>2</sub>TEN dissolved in pyridine was added to a solution of Cu(OAc)<sub>2</sub>·H<sub>2</sub>O in pyridine. A green micro-crystalline precipitate formed that was filtered off and re-crystallized from PY/EtOH to obtain crystals suitable for XRD study.

The complex *trans*-[Cu<sup>II</sup>(*Q,Q'*-MBT)<sub>2</sub>(*N*-PPA)<sub>2</sub>], **15** was obtained through a procedure similar to that above reported for **8** by using HCIN and copper acetate in refluxing MeOH. The crude solid product that formed was collected and then re-crystallized from DMF to produce single crystals suitable for XRD studies. Unexpectedly, those crystals contained complex molecules that have not any HCIN coordinated to the metal; instead, new ligand molecules namely MBT and PPA were found in the coordination sphere (see below comments on the structure).

On summarizing, the general procedure from alcohol solutions of the ligand and alcohol solutions of metal acetate guaranteed high yield for pure compounds suitable for most purposes. In case ultra-pure compounds or single crystals for XRD were needed re-crystallization steps from solvents like DMF, DMSO, PY, gave excellent results.

## 3.2. Structures of the Anti-Inflammatory Drug – Metal Complexes

### 3.2.1. The Coordination Sphere

Complexes of Co(II), Zn(II) and Cd(II) complexes with HMEL<sup>-</sup> anion, **8-10**, have the usual ZZZ conformation for the ligand that chelates *via N*-thiazolyl and *Q*-amide atoms (see Fig. 4 for the structure of **9**). The oxicam anions occupy the equatorial position and have a *trans* arrangement. The solvent molecules (DMSO) are weakly coordinated *via* the oxygen atoms at the apical positions. In the case of Co<sup>II</sup> derivative (**8**) the Co-O and Co-N bond distances at equatorial

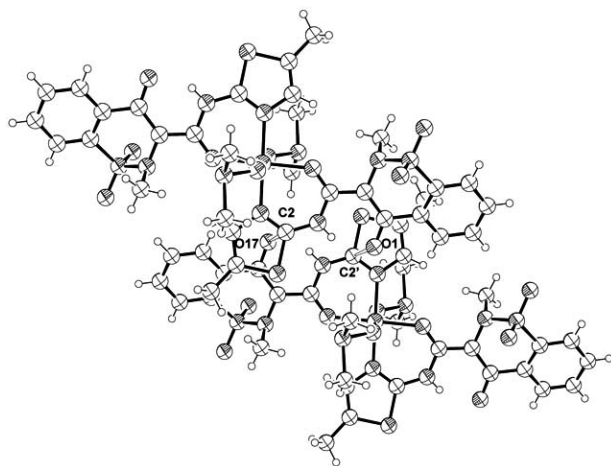


**Fig. (4).** Structure of *trans*-[Zn<sup>II</sup>(*Q,N'*-HMEL)<sub>2</sub>(*Q*-DMSO)<sub>2</sub>], **9** (CSD code, CAKLWU). Inter-molecular stacking interaction between the enolate function (molecule at *x,y,z*) and the thiazolyl ring (molecule at *x,y+1,z*) is evidenced by the short O17...C2' contact distances (3.35(1) Å). The view is almost parallel to the normal for the thiazolyl mean plane.

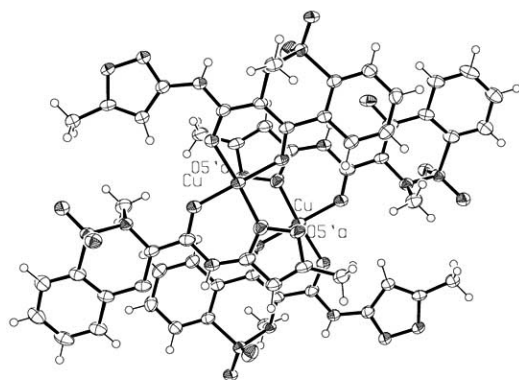
positions are almost the same: 2.083(5) and 2.088(5) Å, respectively. A similar observation can be drawn for the Zn<sup>II</sup> (**9**) and Cd<sup>II</sup> (**10**) derivatives, even though M-N (2.060(6) and 2.254(3) Å) bond lengths seem to be smaller than the M-O (2.081(6) and 2.269(3) Å) ones. For all the three complexes the M-O apical linkages (to DMSO) are significantly weaker than those to the HMEL<sup>-</sup> ligands. Noteworthy, the homologous *trans*-[Cu<sup>II</sup>(*Q,N'*-HPIR)<sub>2</sub>(DMSO)<sub>2</sub>] (**16**) [17] has much stronger Cu-O(amide) linkages (1.942(1) Å) than Cu-N(pyridyl) bonds (2.049(2) Å). As expected the apical linkages to DMSO in the case of the copper complex are much more elongated than for the other structures in the series.

Compound **11** has the usual *pseudo*-octahedral arrangement around the metal (Cd<sup>II</sup>) without the typical significant axial elongations found for the copper derivatives: Cd-O(amide), Cd-N(pyridyl), Cd-O(DMSO) being 2.214(4), 2.302(4), 2.310(4) Å. It has to be noted that in the case of [Cd<sup>II</sup>(*Q,N'*-HPIR)<sub>2</sub>(DMF)<sub>2</sub>] [23] the corresponding distances Cd-O(amide), Cd-N(pyridyl), Cd-O(DMF) are: 2.195(6), 2.276(6) and 2.386(7) Å showing that axial chelation *via* HPIR<sup>-</sup> is stronger than by HTEN<sup>-</sup>, whereas apical coordination by DMF is weaker than by DMSO when the same center is considered (Cd<sup>II</sup>). Chelation angles (amide)O-Cd-N(pyridyl) for **11** measure 81.5(1)° that are close to those for [Cd<sup>II</sup>(*Q,N'*-HPIR)<sub>2</sub>(DMF)<sub>2</sub>] (82.8(2)°).

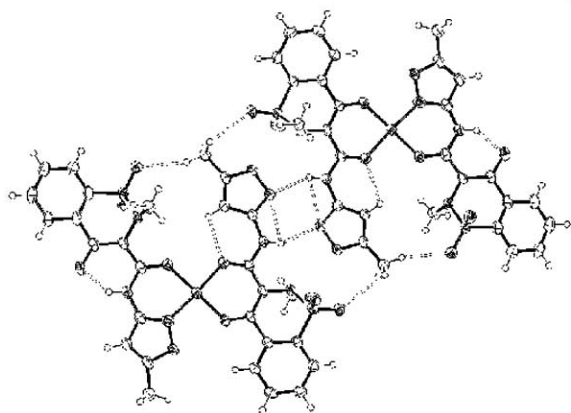
The structure for **12** has a *pseudo*-octahedral arrangement at metal center with a common disposition of the HTEN<sup>-</sup> anions as chelating through amide oxygen and pyridyl nitrogen atoms in the equatorial positions. The two pyridine molecules occupy the apical sites. The Cu-O(amide) (1.934(5) Å) and Cu-N(pyridyl) (2.038(7) Å) bond lengths reveals a preference of metal center for oxygen donor. Even though pyridine is in general quite a good donor for Cu<sup>II</sup> ion, the Cu-N(pyridine) bond is long (2.411(7) Å). This is in agreement with a strong chelating effect by HTEN<sup>-</sup> that stabilizes much the equatorial positions. Noteworthy, the complex was prepared from pyridine and recrystallized from pyridine-ethanol. This suggests that even in the presence of several other strong monodentate ligands, Cu(HOXI)<sub>2</sub> entities are preferably formed.

Just two structures for metal-isoxicam species were reported at our knowledge, namely **13** [16] (Fig. 5) and **17** [17] (Fig. 6). They reveal that the HISO<sup>-</sup> ligand can behave in different manner towards Cu<sup>II</sup> ions. In fact, once the complex obtained from reaction of H<sub>2</sub>ISO and Cu<sup>II</sup>-acetate (in ethanol) is re-crystallized from DMF (**13**), the bis-chelate molecule shows *ambi*-dentate ligating ways for HISO<sup>-</sup>, i.e. one anion chelates *via* enolato oxygen and amide oxygen atoms, and the second anion chelates *via* enolato oxygen and isoxazolyl nitrogen atoms. The complex molecule is tetra-coordinated square-planar and the DMF molecules are just co-crystallized. In the case of the THF derivative (**17**), both the HISO<sup>-</sup> anions chelate through the amide oxygen and isoxazolyl nitrogen atoms. Going back to the structure of **13** and in particular for the *Q,Q'*-chelating molecule the linkage at enolato oxygen is somewhat stronger than that at amide oxygen. In fact, the Cu-O bond distances are 1.884(3) and 1.904(3) Å, respectively. Instead, for the *Q,N'*-chelating molecule, the Cu-O/N bond distances are almost the same 1.915(3) and 1.918(3) Å. Interestingly, in the case of the

octahedral complex **17** the two *Q,N*-chelating HISO<sup>-</sup> anions gives Cu-N and Cu-O bond distances equal to each other (1.950(4) and 1.959(3) Å) but significantly longer than for the DMF derivative. The apical Cu-O(THF) bond distances are much elongated.



(a)



(b)

**Fig. (5).** Representation for two [Cu<sup>II</sup>(*Q,Q*-HISO)(*Q,N*<sup>1+</sup>-HISO)], **13** (CSD code, CIHZID) molecules: (a) stacked, *x,y,z* and  $-x+1,-y+1,-z+1$ ; (b) connected *via* hydrogen bonds, *x,y,z* and  $-x,-y+1,-z$ .

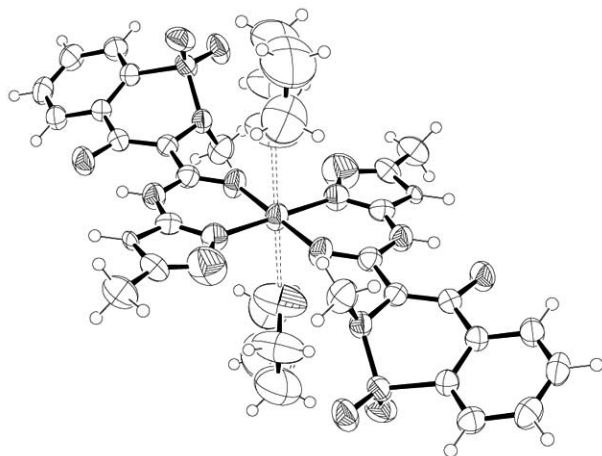
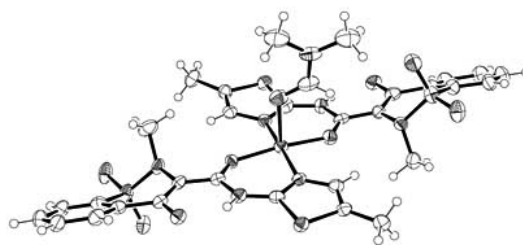


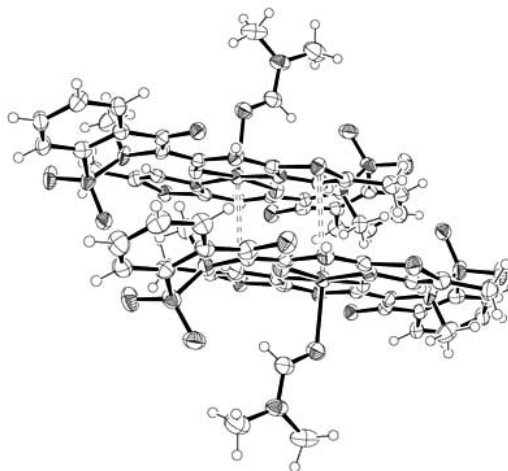
**Fig. (6).** Representation of the molecular structure for *trans*-[Cu(*Q,N*<sup>1+</sup>-HISO)<sub>2</sub>(*Q*-THF)<sub>2</sub>], **17**.

This observations suggest that Cu(HISO)<sub>2</sub> entities can be considered mostly planar molecules with the ability to give very weak apical interactions to the metal. The tendency of apical linkages to dissociate is presumably much higher than that for the equatorial chelating linkages. Furthermore, the nature of the apical ligands as well as the interactions with the bulk modulates the way of interaction with enolato and amide oxygen atoms as well as with amide oxygen and isoxazolyl nitrogen atoms.

The structure for **14** [16] (Fig. 7) is in agreement with most of the previous structures of compounds prepared from alcohol and re-crystallized from weakly coordinating ligands. The metal is bis-chelate by HMEL<sup>-</sup> anions that donates *via* amide oxygen and thiazolyl nitrogen atoms. Interestingly, the metal center has a square-pyramidal arrangement whose apical position is occupied by the oxygen atom from a DMF molecule. The Cu-O(amide) and Cu-N(thiazolyl) bond distances average 1.935(5) and 1.962(5) Å, respectively. The Cu-O apical distance is significantly elongated (2.280(5) Å).



(a)



(b)

**Fig. (7).** (a) View of the complex molecule for *trans*-[Cu(*Q,N*<sup>1+</sup>-HMEL)<sub>2</sub>(*Q*-DMF)], **14** (CSD code, CIHZOJ). (b) View of two complex molecules related by the inversion center at 0.5, 0, 0.5 along a line almost perpendicular to the normal of the coordination planes. The diagram shows that the two square pyramidal basal planes are faced to each other, and that two Cu...S and two stacking interactions that involve mainly the O=C-N(H)-thiazole moieties stabilize the dimer.

The structure of **15** [16] (Fig. 8) reveals that HCIN as such or its anionic form CIN-H16 is not present as ligand in

the complex molecule. It underwent hydrolysis at the ester function, breakage of the amide bond through the nucleophilic attack of methoxy group and the subsequent formation *in situ* of two ligands, namely MBT and PPA that chelate the metal at equatorial positions in a *Q,Q'*-mode and coordinate at apical sites *via* the N-pyridyl atom respectively in a 1:2:2 Cu:MBT:PPA molar ratio. Nevertheless, other mechanistic explanations cannot be ruled out. The Cu-O(enolato), Cu-O(ester, MBT) and Cu-N bond distances are 1.941(1), 1.975(1) and 2.443(2) Å, respectively. The bond angle at metal center are close to idealized values of 90 and 180°.

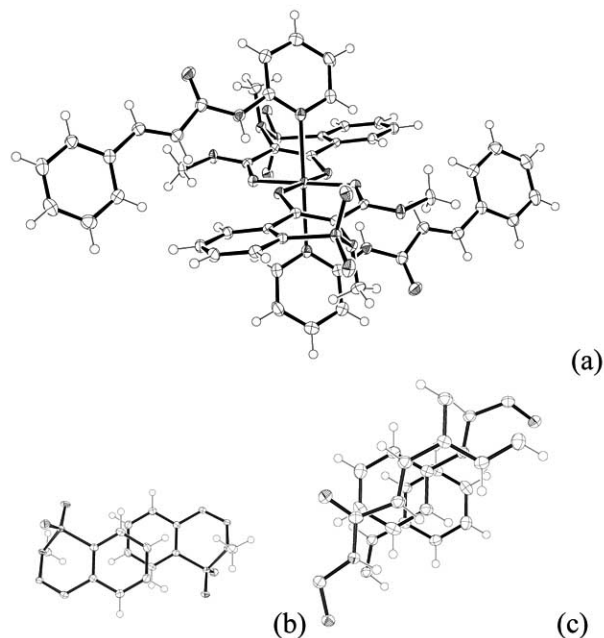


**Fig. (8).** (a) Drawing for the molecular structure of *trans*-[Cu<sup>II</sup>(*Q,Q'*-MBT)<sub>2</sub>(*N*-PPA)<sub>2</sub>], **15** (CSD code, CIHZUP); (b) the diagram shows the stacking interactions that involve the benzothiazine systems from two MBT ligand molecules: left, x,y,z; right, -x+1,-y,-z (shortest inter-atom contact distance: C8...C6, 3.28(1) Å); (c) the diagram shows the stacking interactions that involve two PPA ligand molecules (fragments) (i.e., short inter-atom contact distance: C23...C27, 3.43(1) Å).

### 3.2.2. The Oxycam Ligand

The HOXI<sup>-</sup> ligand for **8-14**, **16**, **17** have a ZZZ conformation. The selected structural parameter for the complexes are listed in Table 4.

Bond distances within the enol/enolato-amide-pyridyl/thiazolyl/oxazolyl chain do not change significantly in the full series of complexes (**8-17**). Bond angles are more sensitive and on increasing the size of metal ions from first row transition metal ions to Cd<sup>II</sup>, the magnitude for C14-N16-C2' angle increases by ca 6°, as well as the N16-C2'-N1' angle decreases by ca the same amount. Deviations from planarity of the atoms along the chain are not large; the magnitudes for ω<sub>17</sub>, ω<sub>15</sub>, ω<sub>4</sub>, ω<sub>3</sub> torsion angles have deviations from idealized values of 0° or 180° not larger than ca 21°.

### 3.2.3. Intra- and Inter-Molecular Weak Interactions

Intra-molecular H-bonds are detectable between O(enolate) and H(N-amide) functions: O...N and H...O distances and angles range 2.51(1)-2.62(1) Å and 138(2)-149(2)° for **8-14**, **16,17**.

As regards inter-molecular H-bond interactions, SO<sub>2</sub> functions for **8-10** are H-acceptors from CH groups (benzo moieties, (DMSO)CH<sub>3</sub>). In the structure of **13**, SO<sub>2</sub> functions are H-acceptors from NCH<sub>3</sub>, (benzo)CH and (isoxazolyl)CH<sub>3</sub> groups. The isoxazolyl oxygen atom is H-acceptor from NCH<sub>3</sub>. The structure of **14** shows inter-molecular H-bond between SO<sub>2</sub> and (benzo)CH, SO<sub>2</sub> and (thiazolyl)CH<sub>3</sub>. Similar interactions occur for the structure of **16** where SO<sub>2</sub> functions accept hydrogen atoms from (pyridyl)CH and (benzo)CH. Finally the structure of **17** has inter-molecular SO<sub>2</sub>...H-C(benzo) interactions.

Amide oxygen atom from PPA (**15**) is H-acceptor from (N)CH<sub>3</sub> groups of MBT. Sulfur dioxide function from MBT is H-acceptor from benzo rings (C...O 3.32(1) Å, H...O 174(2)°).

No appreciable stacking interactions were detected in the series **8-11**. Instead, stacking π...π interactions were detected for **13** [16] (Fig. 5). The almost planar complex molecules are piled along the **a** crystallographic axis. Some interactions involve the benzo system, the enolate-amide chain and isoxazolyl ring. Short contact distances such as (amide)O...N(isoxazolyl) (3.28(1) Å) suggest that stacking forces might be significant. Stacking interactions for **14** were detected and extensively commented in Ref. [16]. Two square-pyramidal complex molecules are set up-down in the crystal and face through the basal plane that consists of two HMEL<sup>-</sup> chelators. Short contacts were detected between thiazolyl and amide functions: C...O 3.45(1) Å. The arrangement causes the (thiazolyl)S atom from a molecule to be located at 3.61(1) Å from Cu<sup>II</sup> in a vacant apical site and *trans* to DMF oxygen atom (S...Cu-O 172.1(5)°). Stacking π...π interactions involve the PPA ligands (**15**) that are piled almost along the **a** axis and involve mostly the styryl and pyridyl functions. The overlap is large, planes are close to be parallel, interatomic contact distances are as short as 3.43(1) Å. Benzo-rings from MBT ligands are involved in π...π stacking interactions characterized by short contacts (i.e. 3.28(1) Å), by a small overlap between planes that are parallel each other. No significant stacking interaction occur in the structure for **16**. Stacking interactions with poor overlap but significant inter-atomic contact distances (as short as 3.41(1) Å) exist in the structure of **17** and involve isoxazolyl and amide systems. Extensive overlap and short contacts characterize the stacking interaction between benzo systems from symmetry related molecules in **17**.

In conclusion the XRD studies for the Werner complexes that contain oxycam ligands clearly shows that the bis-chelating behavior is preferred, no matter what solvent is used for crystal growth. The bis-chelation occurs at the equatorial positions, whereas the apical ligands are weakly bound and can be easily removed. Complex molecules have reasonably high hydrophobicity; in fact, they are neutral and their external surface is rich of hydrophobic functions. Just weak intermolecular C-H...O and π...π forces hold complex molecules together. Thus, it is reasonable to assume that the

**Table 4.** The Selected Bond Distances (Å) and Bond Angles (°) within the HOXI Ligands for Metal Complexes 1-14, 16, 17. Corresponding Data for Complex 15 are also Reported for Comparative Purposes. Estimated Standard Deviations are in the Ranges: 8-11, 16, 17: 0.004-0.008 Å and 0.2-0.5°; 12, 0.010-0.011 Å and 0.7-0.8°; 13 and 14: 0.005-0.009 and 0.3-0.6°; 15, 0.003-0.004 Å and 0.2-0.3°. The CSD [18] Code is also Reported

Parameter	8 CACLOQ	9 CAKLWU	10 CAKMAD	11 HUIMED	12 nd	13 <sup>a</sup> CIHZID	14 CIHZOJ	15 CIHZUP	16 CSD 684972	17 CSD 684973
<b>Distances</b>										
O17-C4	1.264	1.267	1.273	1.264	1.25	1.302/1.285	1.315	1.292	1.265	1.321
C4-C3	1.395	1.394	1.399	1.406	1.42	1.398/1.387	1.380	1.383	1.397	1.365
C3-C14	1.440	1.443	1.431	1.433	1.41	1.426/1.431	1.428	1.439	1.435	1.453
C14-O15	1.248	1.234	1.244	1.252	1.25	1.279/1.272	1.266	1.243	1.256	1.268
C14-N16	1.368	1.371	1.383	1.366	1.36	1.360/1.356	1.350		1.361	1.333
N16-C2'	1.370	1.379	1.371	1.392	1.35	1.361/1.399	1.353		1.380	1.354
<b>Angles</b>										
O17-C4-C3	124.6	124.2	123.8	125.3		122.7/125.4	121.9	125.1	124.4	123.2
C4-C3-C14	123.6	124.3	124.9	124.1		123.1/122.9	123.9	123.3	124.0	123.7
C3-C14-O15	122.5	123.0	122.5	120.6		120.6/123.6	119.7		122.2	118.7
C3-C14-N16	114.4	113.5	113.8	115.5		115.6/118.2	116.9		115.1	114.9
O15-C14-N16	123.1	123.5	123.7	123.8	122.7	123.8/118.2	123.3		122.7	126.4
C14-N16-C2'	127.2	126.1	127.9	133.0	129.4	124.8/124.8	124.9		129.3	120.8
N16-C2'-N1'	127.1	127.0	127.8	121.6		122.7/116.9	127.2		121.6	131.3
<b>Torsion angles</b>										
O17-C4-C3-C14, $\omega_{17}$	0.4	0.8	1.2	3.8		-0.2/6.9	2.9/-1.6	4.6	5.8	1.9
O15-C14-N16-C2', $\omega_{15}$	-9.8	-11.1	-13.2	-6.6		-0.6/-4.8	-3.8/9.1		-10.6	-6.8
C14-N16-C2'-N1', $\omega_{14}$	18.1	19.5	20.9	4.8		0.5/177.0	7.7/-5.6		19.5	2.5
C4-C3-C14-N16, $\omega_4$	-1.1	-1.7	-2.0	-1.9		0.2/172.6	1.5/-1.9		-2.0	7.1
C3-C14-N16-C2', $\omega_3$	169.0	168.4	166.3	174.8		-179.2/175.9	176.3/-170.2		167.2	173.8

<sup>a</sup>Data relevant to the *Q,N*-HISO' ligand are typed first. nd, not deposited.

M(HOXI)<sub>2</sub> entities are significantly inert to incoming ligands from aqueous media. On another side, the apical positions can be ideal to form reversible linkages with carrier systems such as those found *in vivo* or those used as drug delivery materials.

#### 4. BIOLOGICAL ACTIVITY

##### 4.1. Oxygen Radical Scavenger (ORS) Activity

[Cu(*Q,N*<sup>1'</sup>-HPIR)<sub>2</sub>(DMF)<sub>2</sub>] [9,23 and references cited therein] was tested for its ORS activity *via* chemiluminescence methods [24,25]. Noteworthy, the complex was more active than inorganic Cu<sup>II</sup> and than free H<sub>2</sub>PIR. Human neutrophils from healthy subjects and the complex were mixed in DMSO/glycerol/phosphate buffer saline (2:1:2 v/v). The integrated chemiluminescence signals (as a measure of the concentration of residual oxygen radicals) showed that a mixture of the copper complex and H<sub>2</sub>PIR (overall

Cu:H<sub>2</sub>PIR, 1:10 molar ratio) reduces by a factor of ca 8 the concentration of oxygen radicals when compared to the effect caused by H<sub>2</sub>PIR alone. The high ORS activity for Cu(HPIR)<sub>2</sub> suggests a possible stronger anti-inflammatory activity (*via* ORS) by the metal complex when compared to free H<sub>2</sub>PIR and CuCl<sub>2</sub> [24]. This possibility demands that *in vivo* tests against inflammation for all the known metal-oxo complexes are carried out in the next future. A better membrane permeability for M(HOXI)<sub>2</sub> species when compared to H<sub>2</sub>OXI and CuCl<sub>2</sub> is reasonably expected, and might explain the higher ORS ability by the metal complexes.

##### 4.2. Cytotoxic Activity Against Human Cell Cancer Lines and Antibacterial Activity

[Cu(*Q,N*<sup>1'</sup>-HPIR)<sub>2</sub>(DMF)<sub>2</sub>] [9, 23 and references cited therein] was tested for its cytotoxic activity against a panel of human cancer cells at National Cancer Institute, NCI, National Institute of Health NIH, USA, [26], compound code

number NSC# 624662. The panel consisted of ca 50 human cancer cell lines, and showed growth inhibition concentration  $IC_{50}$  values as low as 20  $\mu M$  against several cells. The average  $IC_{50}$  value for the full panel was 54.4  $\mu M$ . The activity was found higher for small cell lung, non-small cell lung, central nervous system, melanoma, ovarian, renal lines. Data deposited at NCI data base showed that *carboplatin* (cis-diammine(1,1-cyclobutanedicarboxylato)platinum(II)) had average  $IC_{50}$  value (101.0  $\mu M$ ), significantly larger than that for  $[Cu(Q,N^1-HPIR)_2(DMF)_2]$  [23]. It has to be recalled that *carboplatin* is currently used world wide against human ovarian cancers. Therefore, owing to the promising activity showed by  $[Cu(Q,N^1-HPIR)_2(DMF)_2]$  [23] it should be of interest testing all the compounds listed in Table 1. A reasonable mechanism for cytotoxic activity for  $M^{II}(HOXI)_2$  compounds, based on spectroscopy measurements was recently proposed [27]. An intercalation into the DNA double helix of the  $M^{II}(HOXI)_2$  species after dissociation of apical ligands is in agreement with the experimental data.

Biological activities originating from  $[SnPh_3(PIR)]$ ,  $[SnPh_3(LOR)]$  and  $[SnPh_3(TEN)]$  complexes have been reported in Ref. [8] and the data have been compared to free ligands and Rifampicin (RMP, as positive drug control). The complexes have been screened as potential drugs against *Mycobacterium tuberculosis* (MT), the pathogenic agent of tuberculosis, and for cytotoxic activity against a selected cancer cell line. The complexes exhibited 100% of inhibitory activity against MT at minimum inhibitory concentration (MIC, lowest concentration of an antimicrobial that completely inhibits the growth of a microorganism after overnight incubation [28]) of 3.13, 1.56 and 0.78  $\mu g/mL$  for lornoxicam, piroxicam and tenoxicam derivatives, respectively. The data are very promising when compared to values found for the free ligands  $H_2TEN$ ,  $H_2PIR$  and  $H_2LOR$  and RMP that showed inhibitory activity against MT of 21, 11, 2 and 95, respectively, and MIC values  $> 6.25 \mu g/mL$  for the three oxicams and 0.25  $\mu g/mL$  for RMP.

The complexes have been also tested for cytotoxicity in Vero cells at concentrations equal to and greater than the MIC value, obtaining  $IC_{50}$  values of 0.07, 0.08 and 0.19  $\mu g/mL$  for  $[SnPh_3(PIR)]$ ,  $[SnPh_3(TEN)]$  and  $[SnPh_3(LOR)]$  complexes, respectively.

On the basis of this reasoning, we stress that more extensive investigations on the biological activities by the metal-compounds as well as on their interactions with bio-molecules and screening *in vitro* and/or *in vivo* seem to be of interest.

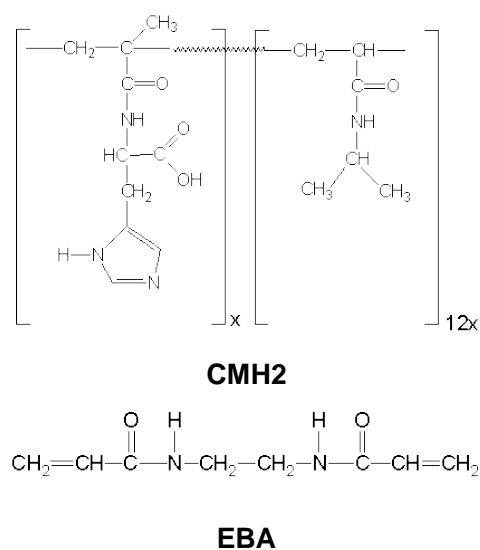
## 5. CARRIER SYSTEMS AND METAL-COMPOUND DELIVERIES

The search of innovative ways to administer drugs mostly in order to avoid undesired side effects attracts the efforts of many workers since a number of years. As examples of carrier systems can be referred: poly-ethylene glycol (PEG), methoxy-ethylene glycol (MEG) [29], mixture of diethylene glycol monoethyl ether (DGME) and propylene glycol monolaurate (PGML) [30], chitosan-based hydrogels [31], hydrogels containing R-amino acid residues (such as L-phenylalanine, L-histidine) [32, 33], silica hydrogels [33] and many others. A small number of studies have been published at our knowledge about oxicam's carrier and delivery

systems, with the aim to decrease the gastro-intestinal side effects and in some cases to increase their therapeutic efficacy [see for example Refs 34 and 35]. The technique to encapsulate the oxicam in host systems, like  $\beta$ -cyclodextrin is one of the studied systems [36]. It is noteworthy that piroxicam is sold as Feldene<sup>®</sup> by Pfizer and as Brexin<sup>®</sup> by Chiesi Farmaceutici SpA. The Brexin<sup>®</sup> takes advantage of the host-guest technology allowing piroxicam to be solubilized by  $\beta$ -cyclodextrin, obtaining a better tolerance by the gastro-intestinal system.

It is predictable that similar tasks will attract deeper attention for metal based drugs that contain metal-oxicam species. A work devoted to the study of a possible way of administering metal-oxicam complexes *via* the usage of synthetic hydrogels in principle implantable into the body after being loaded with drugs is reported in Ref. [17]. The study is based on acrylic hydrogels that are easy to prepare, have low toxicity at least against certain healthy human cells (human osteoblasts), their loading and delivery can be modulated by the nature of certain functionalities grafted into the polymeric chains, by pH, ionic strength, electric potential, temperature, degree of reticulation, etc.

The work showed that the swellable hydrogel, poly(*N*-methacryloyl-L-histidine-*co*-*N*-isopropylacrylamide) cross-linked with *N,N'*-ethylene-bis-acrylamide (EBA, 2%) (named CMH2, Scheme 2), containing histidine residues, isopropyl groups as side chains (1:12 molar ratio), have an acceptable loading ability from DMSO, DMF and THF solutions that contain ca 0.1 M  $Cu(HOXI)_2L_2$  species ( $H_2OXI = H_2PIR, H_2MEL, H_2ISO$  and  $H_2TEN$ ). Once the gel, loaded from DMF or THF, was dried under vacuum in order to remove the solvent and then soaked into aqueous media ( $H_2O$ ,  $H_2O:DMSO$  (90:10, 95:5 or 97:3 v/v), TRIS buffer, citrate/phosphate buffer),  $Cu^{II}(HOXI)_2$  species were released as based on UV and AAS measurements. The amount of complexes released reached concentrations comparable to the  $IC_{50}$  values found for the human cancer cell lines mentioned



**Scheme 2.** Structural formula of hydrogel CMH2, poly(*N*-methacryloyl-L-histidine-*co*-*N*-isopropylacrylamide) (histidine residues:isopropyl groups as side chains, 1:12 molar ratio), cross-linked with *N,N'*-ethylene-bis-acrylamide (EBA, 2%).

above. That happened after a few hours of soaking, in the case the solutions were not renewed at 25°C under stirring for H<sub>2</sub>O:DMSO ca 90:10 v/v (pH 5.6) or TRIS buffer (pH 7.4) (see as example Fig. (9) and Ref. [17] for deeper details).

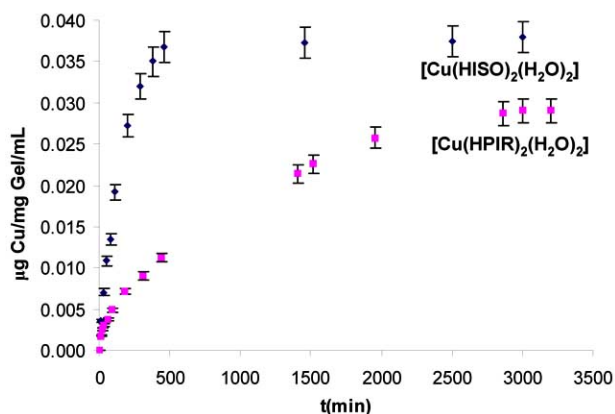


**Fig. (9).** Release measurements as function of time by CMH2 for Cu(HPIR)/Cu(HPIR)<sub>2</sub> and Cu(HISO)/Cu(HISO)<sub>2</sub> in 90:10 (v/v) water/DMSO (pH 5.6).

## 6. CONCLUSION

The review shows that research on new metal-oxicam compounds is quickly expanding as regards synthesis of new species, deep structural and chemical characterization, evaluation of biological properties and investigation on innovative and safe methods for administration *in vivo*. Many more efforts have to be done on the preparative fields in order to study other metal cations never used before, for instance metals from the platinum group metals like Ru, Rh, Ir etc. The studies should look for species characterized by appreciable water solubility. The evaluations of ORS, anti-inflammatory and anti-cancer activities so far systematically performed for just Cu(HPIR)<sub>2</sub> have to be extended to all the chemically characterized compounds, in order to look for structure-activity relationships. More effort towards new strategies for metal-based drug deliveries in physiological media and *in vivo* aimed to reduce the undesired side effects should be also pursued.

## 7. ACKNOWLEDGEMENTS

The author thanks Ministero dell'Università e della Ricerca Scientifica e Tecnologica (MURST, Rome) through PRIN (Progetto di Rilevante Interesse Nazionale) year 2004 (contract n° 2004032118). Thanks are expressed to NCI (National Cancer Institute), USA, for the anticancer tests on [Cu(HPIR)<sub>2</sub>(DMF)<sub>2</sub>] through the Developmental Therapeutics Program (DTP).

## REFERENCES

[1] Savigny P, Kuntze S, Watson P, *et al.* Low back pain: early management of persistent non-specific low back pain. London: National Collaborating Centre for Primary Care and Royal College of General Practitioners. Royal college of general practitioners, 14 Princes Gate, Hyde Park, London, SW7 1PU. www.rcgp.org.uk (2009).

[2] National Center for Health Statistics. Centers for Disease Control and Prevention (Gerberding JL, Director). Health, United States. With Chartbook on Trends in the Health of Americans. Hyattsville: MD 2007.

[3] Chou R, Helfand M, Peterson K, Dana T, Roberts C. Drug Class Review on Cyclo-oxygenase (COX)-2 Inhibitors and Non-steroidal Anti-inflammatory Drugs (NSAIDs). Final Report Update 3, November 2006 produced by Oregon Evidence-based Practice Center Oregon Health & Science University Mark Helfand 2006.

[4] van Haselen RA, Fisher PAG. A randomized controlled trials comparing topical piroxicam gel with a homeopathic gel in osteoarthritis of the knee. *Rheumatology* 2000; 39: 714-9.

[5] Verdina A, Cardillo I, Nebbioso A, *et al.* Molecular analysis of the effects of piroxicam and cisplatin on mesothelioma cell growth and viability. *J Trans Med* 2008; 6: 27-35. <http://www.translational-medicine.com/content/6/1/27>

[6] Ding H, Han C, Gibson-D'Ambrosio R, Steele VE, D'Ambrosio SM. Piroxicam selectively inhibits the growth of premalignant and malignant human oral cell lines by limiting their progression through the S phase and reducing the levels of cyclins and AP-1. *Int J Cancer* 2003; 107: 830-6.

[7] Weder JE, Dillon CT, Hambley TW, *et al.* Copper complexes of non-steroidal anti-inflammatory drugs: an opportunity yet to be realized. *Coord Chem Rev* 2002; 232: 95-126.

[8] Kovala-Demertzi D. Recent advanced on non-steroidal anti-inflammatory drugs, NSAIDs: Organotin complexes NSAIDs. *J Organomet Chem* 2006; 691: 1767-74.

[9] Cini R. Anti-inflammatory compounds as ligands in metal complexes as revealed in X-ray structural studies. *Comments Inorg Chem* 2000; 22: 151-86.

[10] Demertzi MA, Hadjikakou SK, Kovala-Demertzi D, Koutsodimou A, Kubicki M. Organotin-drug interactions. Organotin adducts of tenoxicam: synthesis and characterization of the first organotin complex of tenoxicam. *Helv Chim Acta* 2000; 83: 2787-801.

[11] Galani A, Demertzi MA, Kubicki M, Kovala-Demertzi D. Organotin-drug interactions. Organotin adducts of lornoxicam, synthesis and characterisation of the first complexes of lornoxicam. *Eur J Inorg Chem* 2003; 1761-7.

[12] Defazio S, Cini R. Synthesis, X-ray structural characterization and solution studies of metal complexes containing the anti-inflammatory drugs meloxicam and tenoxicam. *Polyhedron* 2003; 22: 1355-66.

[13] Kovala-Demertzi D, Koutsodimou A, Galani A, *et al.* Diphenylbis(Hpiroxicam)tin(IV), [Ph<sub>2</sub>Sn(Hpir)<sub>2</sub>]. *Appl Organomet Chem* 2004; 18: 501-2.

[14] Defazio S, Cini R. Synthesis, X-ray structure and molecular modelling analysis of cobalt(II), nickel(II), zinc(II) and cadmium(II) complexes of the widely used anti-inflammatory drug meloxicam. *J Chem Soc, Dalton Trans* 2002; 9: 1888-97.

[15] Moya-Hernández MR, Mederos A, Domínguez S, *et al.* Speciation study of the anti-inflammatory drug tenoxicam (Htenox) with Cu(II): X-ray crystal structure of [Cu(tenox)<sub>2</sub>(py)<sub>2</sub>]:EtOH. *J Inorg Biochem* 2003; 95: 131-40.

[16] Cini R, Tamasi G, Defazio S, Hursthouse MB. Unusual coordinating behavior by three non-steroidal anti-inflammatory drugs from the oxicam family towards copper(II). Synthesis, X-ray structure for copper(II)-isoxicam, -meloxicam and -cinnoxicam-derivative complexes, and cytotoxic activity for a copper(II)-piroxicam complex. *J Inorg Biochem* 2007; 101: 1140-52.

[17] Tamasi G, Serinelli F, Consumi M, Magnani A, Casolaro M, Cini R. Release studies from smart hydrogels as carriers for piroxicam and copper(II)-oxicam complexes as anti-inflammatory and anti-cancer drugs. X-ray structures of new copper(II)-piroxicam and -isoxicam complex molecules. *J Inorg Biochem* 2008; 102: 1862-73.

[18] The Cambridge Crystallographic Data Centre CCDC, The Cambridge Structural Database CSD, 12 Union Road, Cambridge, CB2 1EZ, UK. Release January 2009. <http://www.ccdc.cam.ac.uk/products/csd/>

[19] Hadjikakou SK, Demertzi MA, Miller JR, Kovala-Demertzi D. Synthesis and characterization of the first organotin complex of piroxicam. An extended network system *via* non-hydrogen, hydrogen bonding linkages and C-H...π contacts. *J Chem Soc, Dalton Trans* 1999; 5: 663-6.

[20] Cavaglioli A, Cini R. The first X-ray structure of a rhodium complex with the anti-leukemic drug thiopurine. Synthesis, structural characterization and molecular orbital investigation of new rho-

- dium(III) organometallic compounds. *J Chem Soc, Dalton Trans* 1997; 7: 1149-58.
- [21] Di Leo D, Berrettini F, Cini R. Synthesis of platinum(II)-piroxicam compounds. X-ray structure of trans-dichloro( $\eta^2$ -ethene)(piroxicam) platinum(II). *J Chem Soc, Dalton Trans* 1998; 12: 1993-2000.
- [22] Cini R. Synthesis, X-Ray structure and molecular orbital investigation of trans-dichloro (dimethylsulfoxide) (piroxicam) platinum(II). *J Chem Soc, Dalton Trans* 1996; 1: 111-6.
- [23] Cini R, Giorgi G, Cinquantini A, Rossi C, Sabat M. Metal complexes of the antiinflammatory drug piroxicam. *Inorg Chem* 1990; 29: 5197-200.
- [24] Cini R, Pogni R, Basosi R, *et al.* Oxygen radical scavenger activity, EPR, NMR, molecular mechanics and extended-Hückel molecular orbital investigation of the bis(pirosicam)copper(II) complex. *Metal Based Drugs* 1995; 2: 43-56.
- [25] Cini R, Pogni R, Basosi R. EPR and molecular orbital investigation of the superoxide scavenger complex bis(pirosicam)copper(II). *Bull Magn Reson* 1995; 17: 103-7.
- [26] The National Cancer Institute NCI, Developmental Therapeutics Program DTP, The Division of Cancer Treatment & Diagnosis. <http://dtp.nci.nih.gov/> (last updated October 2009).
- [27] Roy S, Banerjee R, Sarkar M. Direct binding of Cu(II)-complexes of oxicam NSAIDs with DNA backbone. *J Inorg Biochem* 2006; 100: 1320-31.
- [28] Andrews JM. Determination of minimum inhibitory concentrations. *J Antimic Chemother* 2001; 48 (Suppl 1): 5-16. Erratum was published on 2002; 49: 1049.
- [28] Popa N, Novac O, Profire L, Lupusoru CE, Popa MI. Hydrogels based on chitosan-xanthan for controlled release of theophylline. *J Mater Sci: Mater Med* 2009 [Epub ahead of print]. doi 10.1007/s10856-009-3937-4.
- [30] Kim T, Kang E, Chun I, Gwak H. Pharmacokinetics of formulated tenoxicam transdermal delivery systems. *J Pharm Pharmacol* 2008; 60: 135-8.
- [31] Bhattarai N, Gunn J, Zhang M. Chitosan-based hydrogels for controlled, localized drug delivery. *Adv Drug Deliv Rev* 2010; 62(1): 83-99.
- [32] Casolaro M, Cini R, Del Bello B, Ferrali M, Maellaro E. Cisplatin/hydrogel complex in cancer therapy. *Biomacromolecule* 2009; 10: 944-9.
- [33] Cini R, Defazio S, Tamasi G, *et al.* Fac- $\{Ru(CO)_3\}^{2+}$ -core complexes and design of metal-based drugs. Synthesis, structure, and reactivity of Ru-Thiazole derivative with serum proteins and absorption-release studies with acryloyl and silica hydrogels as carriers in physiological media. *Inorg Chem* 2007, 46: 79-92.
- [34] Reginster JY, Franchimont P. Piroxicam - beta-cyclodextrin in the treatment of acute pain of rheumatic disease. *Eur J Rheumatol Inflamm* 1993; 12: 38-46.
- [35] Simões S, Marques C, Cruz ME, Martins FMB. Anti-inflammatory effects of locally applied enzyme-loaded ultradeformable vesicles on an acute cutaneous model. *J Microencapsul* 2008; 1-10. [E-pub ahead of print].
- [36] Banerjee R, Chakraborty H, Sarkar M. Host-Guest complexation of oxicam NSAIDs with  $\beta$ -Cyclodextrin. *Biopolymers* 2004, 75: 355-65.

---

Received: December 08, 2009

Revised: January 13, 2010

Accepted: January 14, 2010

© Gabriella Tamasi; Licensee *Bentham Open*.

This is an open access article licensed under the terms of the Creative Commons Attribution Non-Commercial License (<http://creativecommons.org/licenses/by-nc/3.0/>) which permits unrestricted, non-commercial use, distribution and reproduction in any medium, provided the work is properly cited.